

Curving the space by non-Hermiticity

Chenwei Lv^{1,*} Ren Zhang^{2,1,*} and Qi Zhou^{1,3,†}

¹*Department of Physics and Astronomy, Purdue University, West Lafayette, IN, 47907, USA*

²*School of Physics, Xi'an Jiaotong University, Xi'an, Shaanxi 710049, China*

³*Purdue Quantum Science and Engineering Institute,
Purdue University, West Lafayette, IN, 47907, USA*

(Dated: June 7, 2021)

Quantum systems are often characterized into two distinct categories, Hermitian and non-Hermitian ones. Extraordinary properties of non-Hermitian systems, ranging from the non-Hermitian skin effect to the supersensitivity to boundary conditions and perturbations, have been widely explored. Whereas these intriguing phenomena have been considered peculiar to non-Hermitian systems, we show that many of them originate from a duality between non-Hermitian models in flat spaces and their counterparts, which could be Hermitian, in curved spaces. For instance, one-dimensional models with chiral tunnelings are equivalent to their duals in two-dimensional hyperbolic spaces. The dictionary translating between non-Hermiticity and curved spaces delivers an unprecedented routine connecting Hermitian and non-Hermitian physics, unfolds deep geometric roots of non-Hermitian phenomena, and establishes non-Hermiticity as a powerful protocol to engineer exotic curved spaces.

Inevitable system-environment couplings lead to a plethora of intriguing non-Hermitian phenomena [1–7]. Eigenstates are no longer orthogonal and all of them may localize at edges, leading to the non-Hermitian skin effect [8–12]. Whereas Hamiltonians are no longer Hermitian, eigenenergies remain real in certain parameter regimes [13, 14]. At an exceptional point, the energy spectrum may collapse to a single value, resulting in a massive degeneracy and coalesced eigenstates [10, 15, 16]. Changing boundary conditions or adding small perturbations may lead to drastic changes in non-Hermitian systems [17, 18]. These extraordinary properties of non-Hermitian systems have been extensively explored in modern quantum sciences and technologies, ranging from quantum sensing and light harvest to new topological quantum matter [2–5, 7, 19–21].

Since non-Hermitian quantum phenomena appear alien to their Hermitian counterparts, theoretical frameworks for studying non-Hermitian quantum physics often require peculiar tools. To restore orthogonality, left and right vectors that are no longer complex conjugate of each other have been implemented [9, 15, 22]. Metric operators are also introduced to redefine inner products of quantum states in the Hilbert space [23, 24]. However, the physical underlying of these mathematical tools is not clear yet. Moreover, it remains a fundamental challenge to prove that energy spectra of certain non-Hermitian systems are real. Though these systems typically have the \mathcal{PT} symmetry, such a symmetry itself does not guarantee a real energy spectrum and sophisticated mathematical techniques are required [13, 14, 25]. A new approach is desirable for studying non-Hermitian quantum physics and providing more insights to non-Hermitian quantum phenomena.

Here, we show that all aforementioned non-Hermitian phenomena have the same origin, a duality between non-

Hermitian Hamiltonians in flat spaces and their counterparts in curved spaces. While the counterpart could be Hermitian, providing a simple proof of the existence of real energy spectra in non-Hermitian systems, this curved space has an extra dimension, signifying non-Hermitian phenomena as shallows of systems in high dimensions. On the one hand, this duality leads to a new geometric framework providing a unified explanation of many intriguing non-Hermitian phenomena. For instance, the finite curvature delivers an orthonormal condition distinct from that in flat spaces and enforces all eigenstates to localize at the edges. The finite curvature is also the ultimate reason for the supersensitivity to boundary conditions and external perturbations. On the other hand, our duality establishes non-Hermiticity as a unique tool to simulate quantum systems in curved spaces. Since curved spaces often host intriguing quantum phenomena unattainable in their flat counterparts, recent years have witnessed a rapid growth of interest in studying curved spaces [26–29]. However, it remains challenging to engineer curved spaces in laboratories. Our scheme thus provides experimentalists a promising approach of using non-Hermitian systems in flat spaces to manipulate curvatures and create exotic curved spaces that are difficult to access by other means.

The duality between non-Hermiticity and curved spaces can be demonstrated using the celebrated Hatano-Nelson (HN) model [30] and the dual hyperbolic surface. Despite its simplicity, the HN model features all aforementioned intriguing non-Hermitian phenomena, and serves as the basis of a vast range of non-Hermitian models. The HN model reads,

$$-t_R\psi_{n-1} - t_L\psi_{n+1} = E\psi_n, \quad (1)$$

where ψ_n is the eigenstate, E is the eigenenergy, t_L and t_R are the tunneling amplitudes towards the left and the

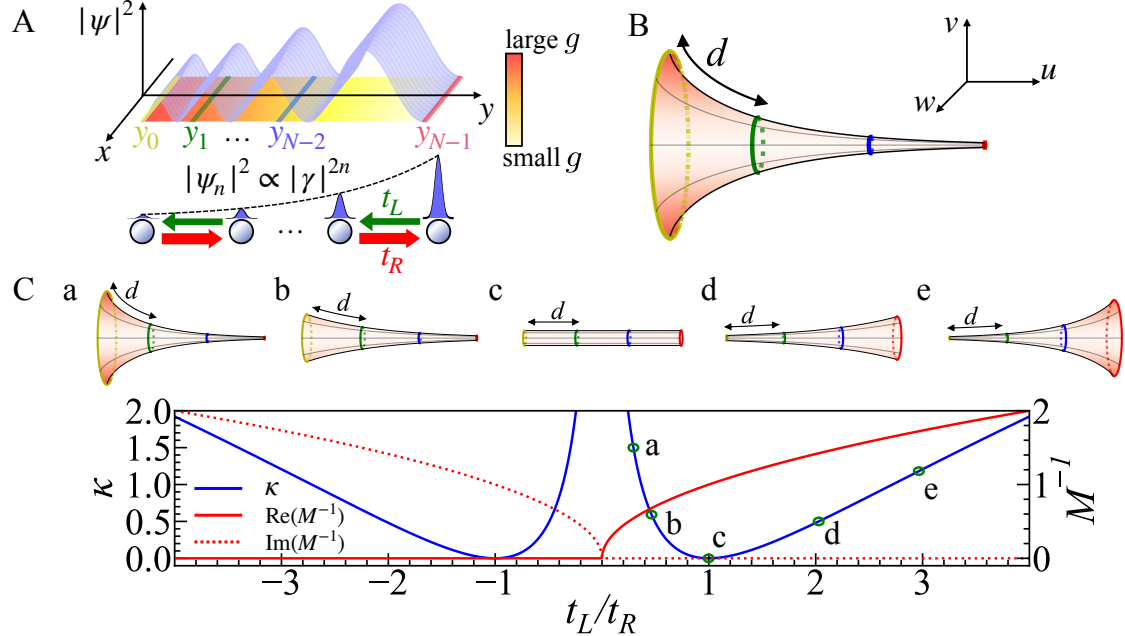


FIG. 1. The duality between the one-dimensional HN model and a hyperbolic surface. (A) A HN chain is mapped to the shaded strip on the Poincaré half-plane, in which an eigenstate with $k_x = 0$ satisfies $|\psi|^2 \propto y$. On the HN chain, eigenstates are localized at the edge, $|\psi_n|^2 \propto |\gamma|^{2n}$. (B) A strip on the Poincaré half-plane with PBC in the x -direction is equivalent to a pseudosphere embedded in three-dimensional Euclidean space. (C) The curvature and the inverse of the effective mass, as functions of t_L for a fixed t_R . The unites of κ and M^{-1} are $1/d^2$ and $2t_Rd^2/(h^2)$, respectively. (a-e) show the dual pseudospheres of the HN model at various $t_L > 0$. A pseudosphere for $t_L < 0$ is the same as that for $-t_L$.

right, respectively. Whenever $t_L \neq t_R^*$, the Hamiltonian becomes non-Hermitian. Such chiral tunnelings can be realized in laboratories using a variety of photonic, electronic, and atomic systems [2, 4, 7, 31, 32]. Eigenstates of the HN model under the open boundary condition (OBC) are written as $\psi_n = \gamma^n \sin(k_m n)/\sqrt{(N+1)/2} \sim e^{n \ln \gamma} \sin(k_m n)$, where $\gamma = \sqrt{t_R/t_L}$, $k_m = m\pi/(N+1)$, $m \in \mathbb{Z}$, and N is the number of lattice sites. Whenever $|\gamma| \neq 1$, all the eigenstates exponentially localize at the right (or left) end of the chain and $1/\ln(|\gamma|)$ defines the localization length. γ^n in ψ_n makes eigenstates with different k_m no longer orthogonal. To restore the orthonormal condition, the so-called left and right vectors $\psi_{L,n} = \psi_n/|\gamma|^{2n}$, $\psi_{R,n} = \psi_n$ need to be defined, $\sum_n \psi_{L,n}^*(k_m) \psi_{R,n}(k_{m'}) = \delta_{m,m'}$ [9, 22].

In the low-energy limit, where the momentum is much smaller than $1/d$ with d being the lattice spacing, Eq. (1) is dual to a continuous model defined in two-dimensional Poincaré half-plane, a prototypical hyperbolic surface. When $t_L, t_R > 0$, the model on the Poincaré half-plane

Hyperbolic space	κ	$\hbar^2/(2M)$	y_{N-1}/y_0
HN model	$4\ln^2(\gamma)/d^2$	$d^2\sqrt{t_R t_L}$	$ \gamma ^{2(N-1)}$

TABLE I. The mapping between parameters of the Poincaré half-plane and the HN model.

is Hermitian. The Schrödinger equation is written as,

$$-\frac{\hbar^2}{2M} \kappa \left(y^2 \nabla^2 + \frac{1}{4} \right) \Psi(x, y) = E \Psi(x, y), \quad (2)$$

where $\nabla^2 = \left(\frac{\partial^2}{\partial x^2} + \frac{\partial^2}{\partial y^2} \right)$, $-\kappa$ is the curvature of the Poincaré half-plane, M is the mass. The metric tensor is $\mathbf{g} = \frac{1}{\kappa y^2} (dx^2 + dy^2)$, $g = \det(\mathbf{g}) = 1/(\kappa^2 d^4)$. Due to the translation symmetry in the x direction, k_x is a good quantum number. As such, the dimension reduction leads to a 1D Schrödinger equation. In particular, when $k_x = 0$, we obtain,

$$-\frac{\hbar^2}{2M} \kappa \left(y^2 \frac{\partial^2}{\partial y^2} + \frac{1}{4} \right) \psi(y) = E \psi(y). \quad (3)$$

The duality between Eq. (1) and Eq. (3) is explicitly shown in Table I, which is a dictionary translating microscopic parameters between these two models. For instance, under OBC, eigenstates of Eq. (3) with eigenenergies of $\kappa \hbar^2 k_y^2/(2M)$ are the low energy limit of that of Eq. (1) with $E_m = -2\sqrt{t_L t_R} \cos(m\pi/(N+1))$. $n = \ln(y/y_0)/(\sqrt{\kappa} d)$ maps eigenstates in the HN model to eigenstates in a Poincaré half-plane, $(y/y_0)^{\frac{1}{2}} \sin(k_y \ln(y/y_0))$, where $k_y = \frac{k_m}{\sqrt{\kappa} d}$. Therefore, a HN model corresponds to a piece of strip in the Poincaré half-plane. The eigenstate of the HN model is equivalent to that in a discrete set of line segments par-

allel to the x axis of a Poincaré half-plane. The separation between adjacent line segments grows exponentially when y increases, as shown in Fig. 1 A.

To derive the duality, we define $\sqrt{d}\psi(s_n) \equiv \psi_n$, where $s_n = nd$ and $n = 0, 1, \dots, N-1$. We also define $\phi(s) \equiv \psi(s)e^{-qs}$ such that $\psi_n = \phi(s_n)e^{qs_n}$. $\phi(s)$ varies slowly with changing s . Substituting ψ_n into Eq. (1) and using the Taylor expansion for $\phi(s)$, $\phi(s_{n\pm1}) = \phi(s_n) \pm d\partial_s\phi + \frac{1}{2}d^2\partial_s^2\phi$, we obtain a Schrödinger equation for $\phi(s)$ in the continuum, $(A + B\partial_s + C\partial_s^2)\phi = E\phi$, where $A = 2C/d^2 = -(t_R e^{-qd} + t_L e^{qd})$, $B/d = t_R e^{-qd} - t_L e^{qd}$. A generic expression for ψ is $e^{iks}e^{qs}$, where both k and q are real and the eigenenergy $E(q+ik)$ is a function of $q+ik$. To enforce OBC, $\psi(0) = \psi((N-1)d) = 0$, $E(q+ik) = E(q-ik)$ is required such that the superposition of $e^{iks}e^{qs}$ and $e^{-iks}e^{qs}$ forms a standing wave. We obtain $B = 0$ and the Schrödinger equation for $\psi(s)$ is written as

$$-\sqrt{t_L t_R} d^2 \left[\left(\frac{\partial}{\partial s} - q \right)^2 + \frac{2}{d^2} \right] \psi(s) = E\psi(s), \quad (4)$$

where $q = d^{-1} \ln \left(\sqrt{\frac{t_R}{t_L}} \right)$. It describes a nonrelativistic particle subject to a purely imaginary vector potential, $|\vec{A}| \sim q$ [30]. Applying a coordinate transformation $\frac{y}{y_0} = e^{2qs}$, and translating parameters using Table I, we obtain Eq. (3) up to a constant energy shift $-2\sqrt{t_L t_R}$. Therefore, this dictionary establishes a duality between a non-Hermitian model in the flat space with a Hermitian one in the curved space. A finite k_x simply adds an additional onsite potential to the HN model,

$$V_n \psi_n - t_R \psi_{n-1} - t_L \psi_{n+1} = E\psi_n, \quad (5)$$

where $V_n = \sqrt{t_L t_R} (2 \ln(\gamma) \gamma^{2n} y_0 k_x)^2$. Without transforming s to y , another representation of the hyperbolic surface is accessed (Supplementary Material). This shows that a purely imaginary vector potential in a flat space is equivalent to a hyperbolic surface. Our approach also applies to generic non-Hermitian models with non-uniform tunnelings corresponding to non-constant curvatures and those including beyond the nearest neighbor tunnelings (Supplementary Material).

Normalizations of eigenstates of Eq. (3) reads

$$\int \frac{dy}{\kappa y^2} \psi_{k_y}^*(y) \psi_{k'_y}(y) = \delta_{k_y, k'_y}. \quad (6)$$

As a common feature of curved spaces, the finite curvature appears in the above equation. It can be understood naturally from the metric of the Poincaré half-plane \mathbf{g} . If we consider a strip defined in the domain $x_0 \leq x \leq x_1$, its width in the x -direction depends on y , $L_x(y) = \frac{1}{\sqrt{\kappa y}}(x_1 - x_0)$. A plane wave traveling in the y -direction must include an extra factor $y^{\frac{1}{2}}$ to guarantee the conservation of particle number.

Another useful visualization of a hyperbolic surface is to embed it in three-dimensional Euclidean space (Supplementary Materials). As shown in Fig. 1 B, unlike a flat space with the periodic boundary condition (PBC) in the x -direction, which leads to a cylinder, PBC applied to a Poincaré half-plane produces a pseudosphere of a funnel shape, since the circumference of the circle with a fixed y changes with changing y . For such a strip whose width is L measured in Euclidean space, the circumferences of the two ends of the funnel are $\frac{L}{\sqrt{\kappa y_0}}$ and $\frac{L}{\sqrt{\kappa y_{N-1}}}$, respectively, where $y_n = y_0 e^{2qnd}$.

In the s -coordinate, Eq. (6) is written as $\int \frac{ds}{\sqrt{\kappa y_0}} e^{-2qs} \psi_{k_y}^*(s) \psi_{k'_y}(s) = \delta_{k_y, k'_y}$. Discretizing and transforming it to the HN model, we obtain,

$$\sum_n |\gamma|^{-2n} \psi_n^*(k_m) \psi_n(k_{m'}) = \delta_{k_m, k_{m'}}. \quad (7)$$

The extra factor is precisely the difference between the left and right vectors defined in non-Hermitian systems. Without this extra factor, one may reach misleading conclusions about particle number conservation such as ghost particles in certain models in high energy physics [33]. The extra factor in Eq. (7) sometimes is referred to as a metric operator to characterize Hilbert spaces [24]. However, metric operators have not been identified as properties of any realistic geometries. Here, the mapping to a curved space establishes an explicit physical interpretation of normalization conditions in non-Hermitian systems, and more importantly, a new routine to manipulate curved spaces. We emphasize that our approach does not require that the energy spectrum is entirely real as in the so-called quasi-Hermitian systems [23]. Generically, spectra in the curved space have both real and complex energies, as shown later.

The dictionary in Table I also allows us to equate the non-Hermitian skin effect to its counterpart, a funneling effect on the Poincaré half-plane that we found recently [34]. Rewriting the eigenstates, $y^{\frac{1}{2}} y^{ik_y}$, using the hyperbolic coordinate, $s = \frac{1}{\sqrt{\kappa}} \ln \left(\frac{y}{y_0} \right)$, the exponential localization of eigenstates becomes clear. The embedding in three dimensions also provides a direct visualization. All eigenstates concentrate near the funneling mouth, the smaller end of the funnel. As such, any initial wavepacket travels toward this funneling mouth. Whereas considering either the Poincaré half-plane or the HN model alone, these two types of skin effects seem disconnected, they are unambiguously unified by the duality between non-Hermitian systems and curved spaces.

Table I shows that when $t_L = t_R$, the Gaussian curvature, $-\kappa$, is zero, meaning that the conventional Hermitian tight binding model corresponds to a flat space. When $t_L \neq t_R$, κ becomes finite. For a given $t_R (> t_L)$, κ increases with decreasing t_L . In other words, increasing the non-Hermiticity makes the space more curved. Meanwhile, y_{N-1}/y_0 increases and the length of the strip in

the y -direction $y_{N-1} - y_0$ grows. Approaching the exceptional point, $t_L \rightarrow 0$, its Gaussian curvature diverges. Since the localization length of the wavefunction in the HN model, $1/\ln(|\gamma|)$, decreases with increasing κ , it is this divergent Gaussian curvature that forces all eigenstates to have a vanishing width and overlap completely with each other. As eigenenergies read $E = \kappa \hbar^2 k_y^2 / (2M)$, and M becomes divergent faster than κ , eigenenergies collapse to zero with a massive degeneracy. As such, all extraordinary phenomena at the exceptional point have a natural geometric interpretation. Whereas y_{N-1}/y_0 changes in this process, the distance between y_0 and y_{N-1} in the hyperbolic space, $s = \int_{y_0}^{y_{N-1}} dy' \frac{1}{\sqrt{\kappa y'}} = (N-1)d$, remains unchanged.

Across the exceptional point, $t_L t_R < 0$, and M becomes purely imaginary. As such, the energy spectrum becomes complex. Whereas the continuous model on the Poincaré half-plane is now non-Hermitian, all previous results of positive $t_L t_R$ still apply provided that $M \rightarrow \pm iM$. More generally, M could be complex once we consider complex t_L and t_R (Supplementary Material). This can be viewed as a particle moving in the hyperbolic space with dissipations. Eigenenergies then become complex and stationary states no longer exist.

Whereas the non-relativistic theory captures dynamics of wavepackets composed of plane waves with small momenta, away from the band bottom (or top), a relativistic theory could be derived (Supplemental Material),

$$-2\sqrt{t_L t_R} [\cos(k_0 d) + k_0 d \sin(k_0 d)] \pm i\sqrt{\kappa} d \sin(k_0 d) \left(\frac{\partial}{\partial y} - \frac{1}{2y} \right) \psi(y) = E \psi(y), \quad (8)$$

where \pm corresponds to the left and right moving wavepackets centered around $\pm k_0$ respectively. Eq. (8) shows that the curvature is independent of k_0 in the HN model. More generically, the curvature varies with changing k_0 if extra terms exist in Hamiltonians (Supplementary Material). Since q , the imaginary part of the momentum, is related to the curvature via $q = \sqrt{\kappa}/2$, our approach provides a geometric interpretation for the so-called generalized Brillouin zone [8, 11, 21, 35, 36]. Whereas q is fixed by t_L/t_R in the HN model, it is, in general, a function of the real part of the momentum, as seen from the energy-dependent κ .

We now consider PBC, under which the eigenstate of Eq. (3) is written as y^{ik_y} . Such an eigenstate has a complex energy for any κ and M , a phenomenon identical to that in the HN model. To understand how such sensitivity to boundary conditions occurs in both models, we first consider the HN model on a lattice ring. Adding an onsite energy offset, $V_L \geq 0$, in one of the lattice sites allows us to continuously change the boundary condition, since an infinite V_L and a vanishing V_L give rise to OBC and PBC, respectively. This is equivalent to adding a superlattice of the lattice spacing N to an infinitely long

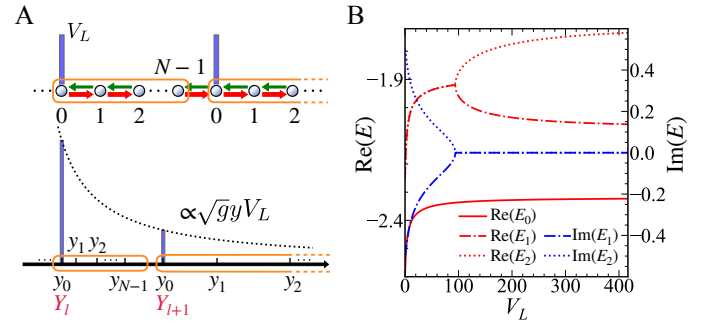


FIG. 2. Changing boundary conditions. (A) In the lattice model, a constant external potential, V_L , is added to the first site in each unit cell of the superlattice. The corresponding external potential in the curved space depends on the position. $V_L = 0(\infty)$ corresponds to the periodic (open) boundary condition. (B) Eigenenergies for the ground state $E_0 \in \mathbb{R}$ and the first two excited states $E_{1,2} \in \mathbb{C}$ as functions of V_L . $\sqrt{t_R/t_L} = 1.5$ and $N = 12$ are used.

chain as shown in Fig. 2 A. The original HN chain corresponds to a single unit cell of this superlattice. Fig. 2 B shows how eigenenergies change as a function of V_L . Using the dictionary in Table I, such a superlattice maps to an external potential added to the dual model in the Poincaré half-plane,

$$V_\delta = dV_L \sqrt{\kappa} y \sum_l \delta(y - Y_l), \quad (9)$$

where Y_l is the lattice site of the superlattice. The y -dependent amplitude of the delta-functions guarantees the scale invariance and each section between Y_l and Y_{l+1} is equivalent. With V_L decreasing from infinity to zero, eigenstates in the Poincaré half-plane evolve from those under OBC to the ones under PBC. $\int_{Y_l^-}^{Y_l^+} \sqrt{g} dy V_\delta \sim 1/\sqrt{\kappa}$ sets the energy scale of the potential, such that the larger the non-Hermiticity is, more sensitive of the system is to the boundary condition.

The duality allows us to use the HN model as a building block to construct exotic curved spaces. Whereas our results can be directly generalized to arbitrary dimensions, here, we use multiple HN chains to illuminate how different inter-chain couplings t may lead to distinct three-dimensional curved spaces. Fig. 3 A and B show two different non-Hermitian models in two dimensions by coupling multiple HN chains. For simplicity, we consider identical HN chains. Our results can be directly generalized to HN chains with different t_L and t_R .

Our duality implies that inter-chain couplings between HN models are mapped to inter-plane couplings between hyperbolic surfaces. The effective theory, for instance, at the band bottom of the case in Fig. 3 A, i.e., $(k_0, k_{z0}) = (0, 0)$, describes a quantum particle with $k_x = 0$ in a

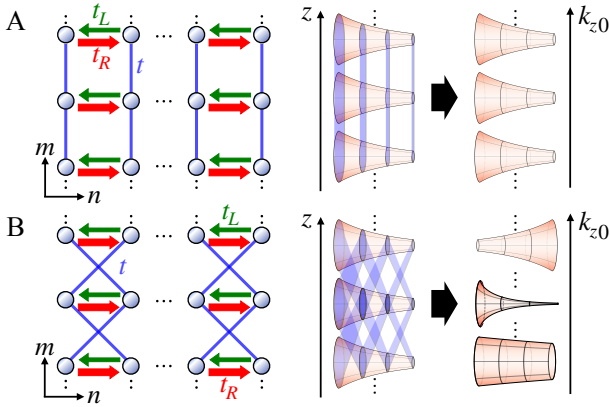


FIG. 3. A set of coupled HN chains is equivalent to a three-dimensional curved space. (A) One-dimensional chains are coupled in parallel and the curvature of each decoupled surface remains unchanged. (B) Diagonal couplings fundamentally influences each curved surface, and the curvature becomes energy-dependent.

three-dimensional curved space,

$$-\left(\sqrt{t_L t_R} d^2 \kappa y^2 \frac{\partial^2}{\partial y^2} + t d^2 \frac{\partial^2}{\partial z^2}\right) \Psi(y, z) = E \Psi(y, z). \quad (10)$$

Since the motions in the y and z directions are decoupled, the wavefunction can be written as $\Psi(y, z) = \psi(y) e^{ik_z z}$. $k_z \neq 0$ adds a constant potential to these Poincaré half-planes and such inter-chain couplings do not change the curvature of any of them. In contrast, the non-relativistic effective theory for Fig. 3 B describes a quantum particle with $k_x = 0$ in a distinct three-dimensional curved space,

$$-\left[\tilde{t} \kappa_c y^2 \frac{\partial^2}{\partial y^2} + \frac{t(t_R - t_L)}{\tilde{t}} \frac{\partial^2}{\partial z^2} \left(\frac{4t + t_R + t_L}{t_R - t_L}\right) + d\sqrt{\kappa_c} \left(y \frac{\partial}{\partial y} - \frac{1}{2}\right)\right] \Psi(y, z) = \frac{E}{d^2} \Psi(y, z), \quad (11)$$

where $\kappa_c = \ln^2 \left(\frac{t_R + 2t}{t_L + 2t}\right) / d^2$, and $\tilde{t} = \sqrt{(t_R + 2t)(t_L + 2t)}$ (Supplementary Material). Such coupled HN chains can be decoupled to independent hyperbolic surfaces, each of which is characterized by a given k_{z0} . Their curvatures depend on both k_{z0} and t (Supplementary Material). While some of these hyperbolic surfaces may be more curved, some others may even become flat due to the couplings. Different hyperbolic surfaces will also experience exceptional points at different values of t and the spectrum includes both real and imaginary eigenenergies. These results show that coupled HN chains provide a unique opportunity to design curved spaces in high dimensions, engineer couplings between curved spaces, and explore how such couplings manipulate curvatures of the spaces.

The duality between non-Hermitian systems and curved spaces provides not only a new perspective to

understand non-Hermitian physics but also a powerful scheme to design exotic curved spaces. Alternatively, experimentalists could use curved spaces that are readily available in laboratories to study non-Hermitian physics in a lower dimension [26–29]. We hope that our work will stimulate more interest in using geometric frameworks to study non-Hermitian physics.

QZ acknowledges useful discussions with Mahdi Hosseini and Pramey Upadhyaya about realizations of chiral couplings. Q. Zhou and C. Lv are supported by the Air Force Office of Scientific Research under award number FA9550-20-1-0221, DOE DE-SC0019202, W. M. Keck Foundation, and a seed grant from PQSEI. R. Zhang is supported by the National Key R&D Program of China (Grant No. 2018YFA0307601), NSFC (Grant No.11804268).

* They contribute equally to this work.

† zhou753@purdue.edu

- [1] N. Syassen, D. M. Bauer, M. Lettner, T. Volz, D. Dietze, J. J. García-Ripoll, J. I. Cirac, G. Rempe, and S. Dürr, Strong dissipation inhibits losses and induces correlations in cold molecular gases, *Science* **320**, 1329 (2008).
- [2] A. Regensburger, C. Bersch, M.-A. Miri, G. Onishchukov, D. N. Christodoulides, and U. Peschel, Parity-time synthetic photonic lattices, *Nature* **488**, 167 (2012).
- [3] L. Feng, Z. J. Wong, R.-M. Ma, Y. Wang, and X. Zhang, Single-mode laser by parity-time symmetry breaking, *Science* **346**, 972 (2014).
- [4] S. Longhi, D. Gatti, and G. D. Valle, Robust light transport in non-Hermitian photonic lattices, *Scientific Reports* **5** (2015), 10.1038/srep13376.
- [5] W. Chen, S. K. Özdemir, G. Zhao, J. Wiersig, and L. Yang, Exceptional points enhance sensing in an optical microcavity, *Nature* **548**, 192 (2017).
- [6] J. Li, A. K. Harter, J. Liu, L. de Melo, Y. N. Joglekar, and L. Luo, Observation of parity-time symmetry breaking transitions in a dissipative floquet system of ultracold atoms, *Nature Communications* **10** (2019), 10.1038/s41467-019-08596-1.
- [7] S. Weidemann, M. Kremer, T. Helbig, T. Hofmann, A. Stegmaier, M. Greiter, R. Thomale, and A. Szameit, Topological funneling of light, *Science* **368**, 311 (2020).
- [8] S. Yao and Z. Wang, Edge states and topological invariants of non-Hermitian systems, *Phys. Rev. Lett.* **121**, 086803 (2018).
- [9] F. K. Kunst, E. Edvardsson, J. C. Budich, and E. J. Bergholtz, Biorthogonal bulk-boundary correspondence in non-Hermitian systems, *Phys. Rev. Lett.* **121**, 026808 (2018).
- [10] V. M. Martinez Alvarez, J. E. Barrios Vargas, and L. E. F. Foa Torres, Non-Hermitian robust edge states in one dimension: Anomalous localization and eigenspace condensation at exceptional points, *Phys. Rev. B* **97**, 121401 (2018).
- [11] K. Zhang, Z. Yang, and C. Fang, Correspondence between winding numbers and skin modes in non-Hermitian systems, *Phys. Rev. Lett.* **125**, 126402 (2020).

[12] N. Okuma, K. Kawabata, K. Shiozaki, and M. Sato, Topological origin of non-Hermitian skin effects, *Phys. Rev. Lett.* **124**, 086801 (2020).

[13] C. M. Bender and S. Boettcher, Real spectra in non-Hermitian Hamiltonians having PT symmetry, *Phys. Rev. Lett.* **80**, 5243 (1998).

[14] A. Mostafazadeh, Pseudo-Hermiticity versus PT symmetry: The necessary condition for the reality of the spectrum of a non-Hermitian Hamiltonian, *Journal of Mathematical Physics* **43**, 205 (2002).

[15] Y. Ashida, Z. Gong, and M. Ueda, Non-Hermitian physics, *arXiv preprint arXiv:2006.01837* (2020).

[16] E. J. Bergholtz, J. C. Budich, and F. K. Kunst, Exceptional topology of non-Hermitian systems, *Rev. Mod. Phys.* **93**, 015005 (2021).

[17] Y. Xiong, Why does bulk boundary correspondence fail in some non-Hermitian topological models, *Journal of Physics Communications* **2**, 035043 (2018).

[18] N. Okuma and M. Sato, Topological phase transition driven by infinitesimal instability: Majorana fermions in non-Hermitian spintronics, *Phys. Rev. Lett.* **123**, 097701 (2019).

[19] J. Wiersig, Enhancing the sensitivity of frequency and energy splitting detection by using exceptional points: Application to microcavity sensors for single-particle detection, *Phys. Rev. Lett.* **112**, 203901 (2014).

[20] K. Kawabata, K. Shiozaki, M. Ueda, and M. Sato, Symmetry and topology in non-Hermitian physics, *Phys. Rev. X* **9**, 041015 (2019).

[21] L. Xiao, T. Deng, K. Wang, G. Zhu, Z. Wang, W. Yi, and P. Xue, Non-Hermitian bulk-boundary correspondence in quantum dynamics, *Nature Physics* **16**, 761 (2020).

[22] D. C. Brody, Biorthogonal quantum mechanics, *Journal of Physics A: Mathematical and Theoretical* **47**, 035305 (2013).

[23] F. Scholtz, H. Geyer, and F. Hahne, Quasi-Hermitian operators in quantum mechanics and the variational principle, *Annals of Physics* **213**, 74 (1992).

[24] A. Mostafazadeh, Pseudo-Hermitian representation of quantum mechanics, *International Journal of Geometric Methods in Modern Physics* **07**, 1191 (2010).

[25] P. Dorey, C. Dunning, and R. Tateo, A reality proof in PT-symmetric quantum mechanics, *Czechoslovak Journal of Physics* **54**, 35 (2004).

[26] T.-L. Ho and B. Huang, Spinor condensates on a cylindrical surface in synthetic gauge fields, *Phys. Rev. Lett.* **115**, 155304 (2015).

[27] R. Bekenstein, Y. Kabessa, Y. Sharabi, O. Tal, N. Engheta, G. Eisenstein, A. J. Agranat, and M. Segev, Control of light by curved space in nanophotonic structures, *Nature Photonics* **11**, 664 (2017).

[28] X.-F. Zhou, C. Wu, G.-C. Guo, R. Wang, H. Pu, and Z.-W. Zhou, Synthetic landau levels and spinor vortex matter on a haldane spherical surface with a magnetic monopole, *Phys. Rev. Lett.* **120**, 130402 (2018).

[29] A. J. Kollár, M. Fitzpatrick, and A. A. Houck, Hyperbolic lattices in circuit quantum electrodynamics, *Nature* **571**, 45 (2019).

[30] N. Hatano and D. R. Nelson, Non-Hermitian delocalization and eigenfunctions, *Phys. Rev. B* **58**, 8384 (1998).

[31] P. Lodahl, S. Mahmoodian, S. Stobbe, A. Rauschenbeutel, P. Schneeweiss, J. Volz, H. Pichler, and P. Zoller, Chiral quantum optics, *Nature* **541**, 473 (2017).

[32] S.-H. Yang, R. Naaman, Y. Paltiel, and S. S. P. Parkin, Chiral spintronics, *Nature Reviews Physics* **3**, 328 (2021).

[33] C. M. Bender, S. F. Brandt, J.-H. Chen, and Q. Wang, Ghost busting: \mathcal{PT} -symmetric interpretation of the lee model, *Phys. Rev. D* **71**, 025014 (2005).

[34] R. Zhang, C. Lv, Y. Yan, and Q. Zhou, Efimov-like states and quantum funneling effects on synthetic hyperbolic surfaces, *arXiv preprint arXiv:2010.05135* (2020).

[35] K. Yokomizo and S. Murakami, Non-bloch band theory of non-Hermitian systems, *Phys. Rev. Lett.* **123**, 066404 (2019).

[36] Z. Yang, K. Zhang, C. Fang, and J. Hu, Non-Hermitian bulk-boundary correspondence and auxiliary generalized Brillouin zone theory, *Phys. Rev. Lett.* **125**, 226402 (2020).

Supplementary Materials for “Curving the space by non-Hermiticity”

The duality between 2D curved spaces and 1D imaginary vector potentials

The metric tensor of a generic two-dimensional Riemannian surface is written as

$$\mathbf{g} = g_{ij} dx^i dx^j = e^{2\mu(x,y)} (dx^2 + dy^2). \quad (\text{S1})$$

A non-relativistic quantum particle on this Riemannian surface is described by the Schrödinger equation,

$$\frac{\hbar^2}{2M} \left(-\frac{1}{\sqrt{g}} \partial_i g^{ij} \sqrt{g} \partial_j - 4\lambda\kappa \right) \Psi(x, y) = E\Psi(x, y), \quad (\text{S2})$$

where $g = \det(\mathbf{g})$, $-\kappa$ is the Gaussian curvature and in general depends on (x, y) . λ is a coupling constant. We adopt $\lambda = 1/16$ such that the energy spectrum is $[0, \infty)$ for hyperbolic space [1]. A metric tensor that only depends on y allows the dimension reduction to 1D. If we further consider a transformation, $s = \int e^{\nu(y)} dy$, we obtain $\mathbf{g} = e^{2\mu(s)-2\nu(s)} (e^{2\nu(s)} dx^2 + ds^2)$. Using this metric, the Gaussian curvature is obtained,

$$-\kappa = -e^{2\nu-2\mu} (\mu'' + \mu'\nu'), \quad (\text{S3})$$

where μ' and μ'' are the first and the second derivatives with respect to s , respectively. In (x, s) coordinates, Eq. (S2) is rewritten as

$$-\frac{\hbar^2}{2M} e^{2\nu-2\mu} \left[\frac{\partial^2}{\partial s^2} + \nu' \frac{\partial}{\partial s} + e^{-2\nu} \frac{\partial^2}{\partial x^2} + \frac{1}{4} (\mu'' + \mu'\nu') \right] \Psi(x, s) = E\Psi(x, s). \quad (\text{S4})$$

Consider a strip in the (x, s) coordinate with a periodical boundary condition in the x -direction, the wavefunction is written as $\Psi(x, s) = \psi(s) e^{ik_x x}$, where k_x denotes the momentum in the x -direction. $\psi(s)$ satisfies the following 1D Schrödinger equation,

$$-\frac{\hbar^2}{\sqrt{2m(s)}} \left(\frac{\partial}{\partial s} + i \frac{e}{\hbar} A(s) \right)^2 \frac{1}{\sqrt{2m(s)}} \psi(s) + V(s) \psi(s) = E\psi(s), \quad (\text{S5})$$

where c is the speed of light, $-e$ is the charge of quantum particle,

$$m(s) = M e^{2\mu-2\nu}, \quad A(s) = -i \frac{c\hbar}{e} (\mu' - \nu'/2), \quad V(s) = \frac{\hbar^2}{2M} e^{-2\mu} k_x^2 - \frac{\hbar^2}{8M} e^{2\nu-2\mu} (\mu'' - 2\nu'' + \mu'\nu' - \nu'^2). \quad (\text{S6})$$

We would like to point out that Eq. (S5) is the Schrödinger equation for a one-dimensional system with a position-dependent mass $m(s)$, an imaginary vector potential $A(s)$ and an external potential $V(s)$.

When $\mu = \nu$, the mass term becomes a constant, and $A(s) = -i \frac{c\hbar}{e} \frac{\mu'}{2}$, $V(s) = \frac{\hbar^2}{2M} e^{-2\mu} k_x^2 + \frac{\hbar^2}{8M} \mu''$. If we consider $\mu(s) = -2qs$, we find that $V(s) = \frac{\hbar^2}{2M} e^{4qs} k_x^2$, and the imaginary vector potential A becomes a constant, $i \frac{e}{\hbar} A(s) = -q$. The Schrödinger equation becomes,

$$-\frac{\hbar^2}{2M} \left(\frac{\partial}{\partial s} - q \right)^2 \psi(s) + \frac{\hbar^2}{2M} e^{4qs} k_x^2 \psi(s) = E\psi(s). \quad (\text{S7})$$

From the mapping in Table I in the main text and $k_x = 0$, Eq. (4) in the main text is obtained. Moreover, applying Eq. (S3) we get $\kappa = 4q^2$, which defines a surface with a constant negative Gaussian curvature.

Non-Hermitian models with non-uniform tunnelings

In this section, we show that generic non-Hermitian lattice models with non-uniform tunnelings lead to non-constant curvatures. The Schrödinger equation of such a non-Hermitian lattice model is written as

$$-t_{R,n} \psi_{n-1} - t_{L,n} \psi_{n+1} + V_{\text{lattice},n} \psi_n = E\psi_n, \quad (\text{S8})$$

where $t_{R(L),n}$ and $V_{\text{lattice},n}$ change slowly. The dual model in the curved space is written as

$$\frac{\hbar^2}{2M} \left(-\frac{1}{\sqrt{g}} \partial_i g^{ij} \sqrt{g} \partial_j - \frac{\kappa}{4} + V_c(s) \right) \Psi(x, s) = E \Psi(x, s), \quad \mathbf{g} = e^{2\mu(s)} dx^2 + e^{2(\mu(s) - \nu(s))} ds^2, \quad (\text{S9})$$

where $\mu(s)$, $\nu(s)$ and $V_c(s)$ are

$$\begin{aligned} \mu(s = s_n) &= \frac{1}{2} \ln \left(\sqrt{t_{R,n} t_{L,n}} \frac{2M d^2}{\hbar^2} \right) - \sum_{j=1}^n \ln \left(\frac{t_{R,j}}{t_{L,j-1}} \right), \\ \nu(s = s_n) &= \ln \left(\sqrt{t_{R,n} t_{L,n}} \frac{2M d^2}{\hbar^2} \right) - \sum_{j=1}^n \ln \left(\frac{t_{R,j}}{t_{L,j-1}} \right), \\ V_c(s = s_n) &= V_{\text{lattice},n} - V(s_n) - 2\sqrt{t_{R,n} t_{L,n}}, \end{aligned} \quad (\text{S10})$$

where $s_n = nd$.

To prove this duality, we consider $\Psi(s, x) = \psi(s) e^{ik_x x}$ in Eq. (S9) and obtain a 1D model with an imaginary vector potential and a spatial-dependent mass using the approach discussed in the previous section. Then we define $\sqrt{d}\psi(s = s_n) \equiv \psi_n$ and $\phi(s) = e^{\nu/2}\psi(s)$, where $\phi(s)$ is a slowly varying wavefunction such that $\phi(s_{n\pm 1}) \approx \phi(s_n) \pm d\partial_s \phi + \frac{1}{2}\partial_s^2 \phi$. Discretizing the Hamiltonian in which κ is, in general, spatially variant, the Schrödinger equation for ϕ_n becomes

$$-\frac{\hbar^2}{2M d^2} e^{2\nu_n - 2\mu_n} (\phi_{n-1} + \phi_{n+1} - 2\phi_n) + (V_n + V_{c,n})\phi_n = E\phi_n, \quad (\text{S11})$$

where $\nu_n = \nu(s_n)$, $\mu_n = \mu(s_n)$, $V_{c,n} = V_c(s_n)$ and $V_n = V(s_n)$. Correspondingly, the Schrödinger equation for ψ is written as

$$-\frac{\hbar^2}{2M d^2} e^{2\nu_n - 2\mu_n} \left(e^{\nu_{n-1}/2 - \nu_n/2} \psi_{n-1} + e^{\nu_{n+1}/2 - \nu_n/2} \psi_{n+1} - 2\psi_n \right) + (V_n + V_{c,n})\psi_n = E\psi_n. \quad (\text{S12})$$

Substituting Eq. (S10) into Eq. (S12), we obtain Eq. (S8). In the derivation, $|1 - \frac{t_{R(L),n-1}}{t_{R(L),n}}| \ll 1$ has been used for slowly changing $t_{R(L),n}$.

For a special case that

$$\mu = \frac{1}{2} \ln \left(\frac{2M d^2}{\hbar^2} \sqrt{t_R t_L} f(s) \right) - \ln \left(\frac{t_R}{t_L} \right) \frac{s}{d}, \quad \nu = \ln \left(\frac{2M d^2}{\hbar^2} \sqrt{t_R t_L} f(s) \right) - \ln \left(\frac{t_R}{t_L} \right) \frac{s}{d}, \quad V_c = -V(s) - 2\sqrt{t_R t_L} f(s), \quad (\text{S13})$$

where $f(s) = \sqrt{(L + \frac{1}{2})^2 - \frac{s^2}{d^2}}$, Eq. (S12) is written as

$$-\left(t_R \sqrt{L(L+1) - n(n-1)} \psi_{n-1} + t_L \sqrt{L(L+1) - n(n+1)} \psi_{n+1} \right) = E\psi_n, \quad (\text{S14})$$

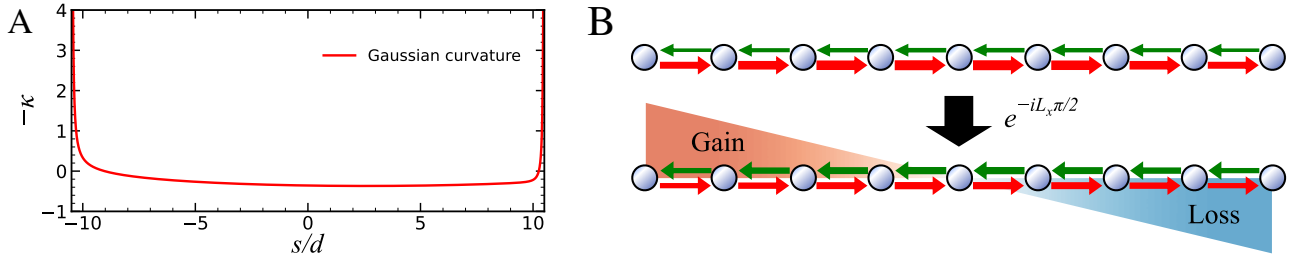


FIG. S1. (A) The Gaussian curvature $-\kappa(s)$ in the unit of $1/d^2$ defined in Eq. (S3) as function of s for the curved space defined in Eq. (S13). We choose $\hbar^2/(2M d^2) = \sqrt{t_R t_L} L$. $L = 10$ and $t_R/t_L = 9/5$ are used in the numerics. (B) A unitary transformation transforms the lattice dual model into a lattice model with Hermitian tunneling terms and on-site gains or losses.

with $n = s/d$. This Schrödinger equation describes a spin- L subject to a complex magnetic field, $\vec{B} = (t_L + t_R)\mathbf{e}_x + i(t_L - t_R)\mathbf{e}_y$. Applying a unitary transformation, $\hat{L}_y \leftrightarrow \hat{L}_z$, Eq. (S14) is mapped to,

$$-\frac{1}{2}(t_L + t_R) \left(\sqrt{L(L+1) - n(n-1)}\psi_{n-1} + \sqrt{L(L+1) - n(n+1)}\psi_{n+1} \right) - i(t_L - t_R)n\psi_n = E\psi_n. \quad (\text{S15})$$

As shown by Fig. S1 B, tunneling terms in this model become Hermitian, while onsite energies become purely imaginary and increase linearly as n grows. Fig. S1 A also shows how the curvature of the dual model to Eq. (S14) changes spatially.

The HN model with the next-nearest-neighbor hopping

In the presence of a next-nearest-neighbor hopping in the HN model, a simple similarity transformation does not exist anymore to map the model to the conventional tight-binding model with Hermitian tunnelings. Nevertheless, the duality to the curved space still exists. The Schrödinger equation of such a model is written as

$$-t'_R\psi_{n-2} - t'_L\psi_{n+2} - t_R\psi_{n-1} - t_L\psi_{n+1} = E\psi_n, \quad (\text{S16})$$

A generic solution to this Schrödinger equation is written as β^n , with eigenenergy $E(\beta) = -(t'_R\beta^{-2} + t'_L\beta^2 + t_R\beta^{-1} + t_L\beta)$. We consider the open boundary condition, $\psi_{n<0} = \psi_{n>N-1} = 0$. As such, the Schrödinger equation formally becomes different near the edges,

$$\begin{aligned} -t'_L\psi_2 - t_L\psi_1 &= E\psi_0, & -t'_L\psi_3 - t_R\psi_0 - t_L\psi_2 &= E\psi_1, \\ -t'_R\psi_{N-3} - t_R\psi_{N-2} &= E\psi_{N-1}, & -t'_R\psi_{N-4} - t_R\psi_{N-3} - t_L\psi_{N-1} &= E\psi_{N-2}. \end{aligned} \quad (\text{S17})$$

Alternatively, the boundary condition can be written as $\psi_{-1} = \psi_{-2} = \psi_N = \psi_{N+1} = 0$.

For a given complex energy E , $t'_L\beta^4 + t_L\beta^3 + E\beta^2 + t_R\beta + t'_R = 0$ has four solutions, denoted by $|\beta_1| \leq |\beta_2| \leq |\beta_3| \leq |\beta_4|$. A specific solution to boundary conditions Eq. (S17) is written as

$$\psi_n = c_1\beta_1^n + c_2\beta_2^n + c_3\beta_3^n + c_4\beta_4^n, \quad (\text{S18})$$

It is known that $|\beta_1| \leq |\beta_2| = |\beta_3| \leq |\beta_4|$ is required to satisfy the boundary condition when $N \rightarrow \infty$. This leads to the definition of the generalized Brillouin zone (GBZ) [2–4]. As such, β_2^n and β_3^n are dominant in the bulk.

Using β_2 and β_3 , we could formulate the effective theory in the bulk. We denote β_2 by $e^{(q+ik_0)d}$ and β_3 by $e^{(q+ik_1)d}$ where q , k_0 and k_1 are real. Using the same method discussed in the main text, we define $\sqrt{d}\psi(s_n) \equiv \psi_n$, $\psi(s) = \phi_0(s)e^{ik_0 s}e^{qs} = \tilde{\psi}_0(s)e^{ik_0 s}$ such that $\phi_0(s)$ is slowly varying with changing s , the Schrödinger equation in the continuum is written as

$$\left[A(k_0) + B(k_0) \frac{\partial}{\partial s} + C(k_0) \frac{\partial^2}{\partial s^2} \right] \phi_0(s) = E\phi_0(s), \quad (\text{S19})$$

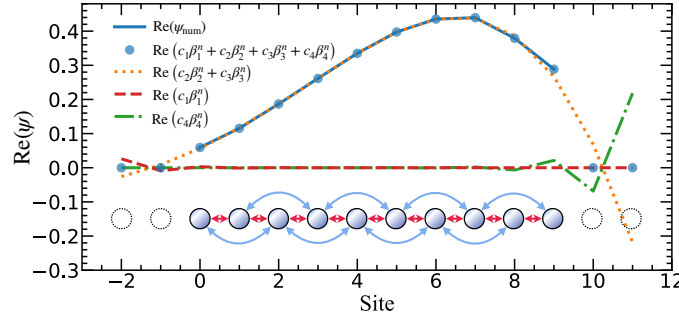


FIG. S2. An eigenstate of the HN model with the next nearest neighbor tunnelings. We use $N = 10$, $t_R = 1$, $t_L = 0.5$, $t'_R = 0.6$, and $t'_L = 0.4$. The real parts of wavefunction are shown and the imaginary parts vanish. The numerical solution is extrapolated to the lattice sites -1 , -2 , 10 and 11 by $\psi_{\text{num}} = c_1\beta_1^n + c_2\beta_2^n + c_3\beta_3^n + c_4\beta_4^n$. Here, $c_2\beta_2^n + c_3\beta_3^n$ forms a standing wave, $c_1\beta_1^n$ and $c_4\beta_4^n$ are localized at the boundary to fulfill the boundary condition.

where

$$\begin{aligned} A(k_0) &= -(t'_R e^{-2(q+ik_0)d} + t'_L e^{2(q+ik_0)d} + t_R e^{-(q+ik_0)d} + t_L e^{(q+ik_0)d}), \\ B(k_0) &= -(-2t'_R e^{-2(q+ik_0)d} + 2t'_L e^{2(q+ik_0)d} - t_R e^{-(q+ik_0)d} + t_L e^{(q+ik_0)d})d, \\ C(k_0) &= -(4t'_R e^{-2(q+ik_0)d} + 4t'_L e^{2(q+ik_0)d} + t_R e^{-(q+ik_0)d} + t_L e^{(q+ik_0)d})d^2/2. \end{aligned} \quad (\text{S20})$$

Since q has been determined by k_0 in GBZ, $A(k_0)$, $B(k_0)$, $C(k_0)$ are known. When $B(k_0) \neq 0$, the effective theory becomes $[A(k_0) + B(k_0) (\frac{\partial}{\partial s} - q)] \tilde{\psi}_0(s) = E\tilde{\psi}_0(s)$. A coordinate transformation $y/y_0 = e^{2qs}$ leads to

$$\left[A(k_0) + 2qB(k_0)y \left(\frac{\partial}{\partial y} - \frac{1}{2y} \right) \right] \tilde{\psi}_0(y) = E\tilde{\psi}_0(y). \quad (\text{S21})$$

Similarly, using β_3 , we obtain,

$$\left[A(k_0) + 2qB(k_1)y \left(\frac{\partial}{\partial y} - \frac{1}{2y} \right) \right] \tilde{\psi}_1(y) = E\tilde{\psi}_1(y), \quad (\text{S22})$$

where $A(k_0) = A(k_1)$ has been used. Both of the above two equations are effective theories for particles with linear dispersions on a Poincaré half-plane, $\hat{H} = -v_f \sqrt{\kappa} \frac{1}{2} (y\hat{p}_y + \hat{p}_y y) = i\hbar v_f \sqrt{\kappa} y \left(\frac{\partial}{\partial y} - \frac{1}{2y} \right)$, where v_f is the Fermi velocity and $\hat{p}_y = \frac{\hbar}{i} \left(\frac{\partial}{\partial y} - \frac{1}{y} \right)$, $\hat{p}_x = \frac{\hbar}{i} \frac{\partial}{\partial x}$. Comparing this Hamiltonian with that in Eq. (S21, S22), we obtain

$$-\kappa = -4q^2, \quad i\hbar v_{f,0} = B(k_0), \quad i\hbar v_{f,1} = B(k_1). \quad (\text{S23})$$

The Fermi velocity thus depends on B . It is also worth mentioning that q is, in general, a function of k_0 . The curvature $-\kappa$ thus also depends on k_0 . When $t'_{L(R)}$ vanish, q is constant fixed by t_L and t_R , and the curvature $-\kappa$ is also a constant independent of the energy, as discussed in the main text.

When $\beta_2 = \beta_3$, we obtain $B(k_0) = 0$ and a non-relativistic effective theory $[A(k_0) + C(k_0) (\frac{\partial}{\partial s} - q)^2] \tilde{\psi}(s) = E\tilde{\psi}(s)$. Comparing it with Eq. (S7), we conclude that $-\kappa = -4q^2$ and the mass term $\frac{\hbar^2}{2M} = -C(k_0)$.

Away from the band bottom (top) of the HN model

Setting $t'_R = t'_L = 0$ in the previous section, we obtain $A(k_0) = -(t_R e^{-(q+ik_0)d} + t_L e^{(q+ik_0)d})$, $B(k_0) = (t_R e^{-(q+ik_0)d} - t_L e^{(q+ik_0)d})d$, and $B(k_1) = (t_R e^{-(q+ik_1)d} - t_L e^{(q+ik_1)d})d$. Using $A(k_1) = A(k_0)$, we find $k_0 = -k_1$ and $e^{qd} = \sqrt{\frac{t_R}{t_L}}$. Therefore, $-\kappa = -4 \ln \left(\sqrt{\frac{t_R}{t_L}} \right)^2 / d^2$ which is independent of k_0 . The Fermi velocity becomes $v_f = \pm 2\hbar^{-1} \sin(k_0 d) d \sqrt{t_R t_L}$. Using $A(k_0)$, $B(k_0)$, $B(k_1)$ in Eq. (S21, S22), and apply $\tilde{\psi}_0 = \psi_0 e^{-ik_0 s}$, $\tilde{\psi}_1 = \psi_1 e^{-ik_1 s}$, we obtain Eq. (8) in the main text.

Poincaré half-plane and pseudosphere

A pseudosphere is a standard visualization of the curved space with a constant negative curvature. It is a two-dimensional surface embedded in a three-dimensional Euclidean space, where each point on this surface is a saddle point. Therefore, the Gaussian curvature equals a negative constant. We define the three-dimensional Euclidean space by $(u, v, w) \in \mathbb{R}^3$. A parameterization of the pseudosphere is

$$(u(\eta, \varphi), v(\eta, \varphi), w(\eta, \varphi)) = \left(R(\eta - \tanh(\eta)), R \frac{\cos(\varphi)}{\cosh(\eta)}, R \frac{\sin(\varphi)}{\cosh(\eta)} \right), \quad (\text{S24})$$

where $\eta > 0$, $\varphi \in (-\pi, \pi)$. R is a constant, which can be understood as the radius of the pseudosphere with Gaussian curvature $-1/R^2$. The induced metric on the pseudosphere is written as

$$g = [(\partial_\eta u)^2 + (\partial_\eta v)^2 + (\partial_\eta w)^2] d\eta^2 + [(\partial_\varphi u)^2 + (\partial_\varphi v)^2 + (\partial_\varphi w)^2] d\varphi^2 = R^2 \tanh(\eta)^2 d\eta^2 + \frac{R^2 d\varphi^2}{\cosh(\eta)^2}. \quad (\text{S25})$$

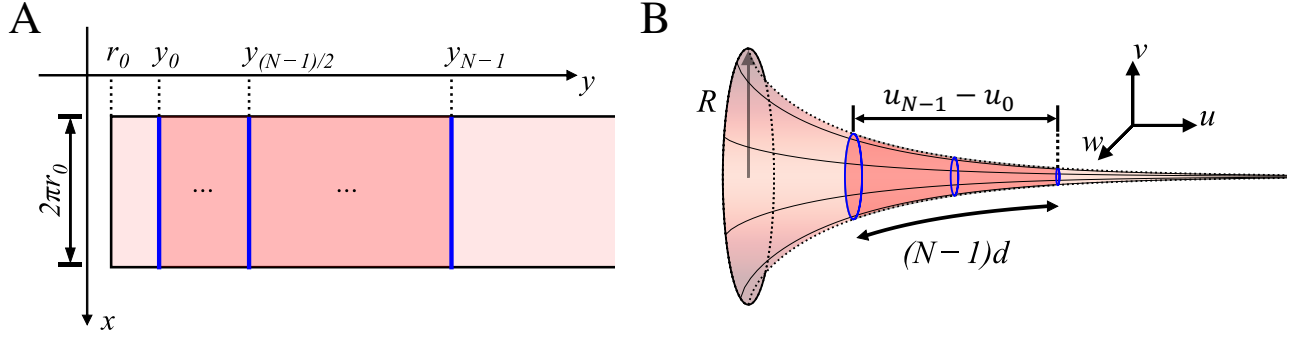


FIG. S3. A strip on the Poincaré half-plane with periodical boundary condition (A) is mapped to a pseudosphere (B) embedded in the Euclidean space $(u, v, w) \in \mathbb{R}^3$ using Eq. (S24,S26). r_0 is mapped to the mouth of the pseudosphere.

If we define

$$y = r_0 \cosh(\eta), \quad x = r_0 \varphi, \quad (\text{S26})$$

where r_0 is an arbitrary constant, and apply periodical boundary condition on the x -direction, the metric tensor Eq. (S25) becomes $\mathbf{g} = \frac{R^2}{y^2} (dx^2 + dy^2)$, which is precisely the metric tensor of the Poincaré half-plane. The pseudosphere is thus mapped to a strip on the Poincaré half-plane.

The lattice spacing d measured by the metric and the radius of the pseudosphere R are obtained from the Table I of the main text, where $d^2 = 2M/(\sqrt{t_R t_L} \hbar^2)$. $d/R = \ln(t_R/t_L) = 2 \ln(\gamma)$ and $y \in (y_0, y_{N-1})$, $y_{N-1}/y_0 = \gamma^{2N-2}$. We choose $r_0 = \xi e^{(N-1)d/(2R)}/R$ for a constant ξ , such that the radius at $y_{(N-1)/2}$, the middle of HN model mapped on the pseudosphere, is fixed during the mapping as ξ/y_0 . With this parameterization, as shown by Fig. S3 B, we have

$$(u_{N-1} - u_0)/d = \frac{1}{2 \ln(\gamma)} \left[\operatorname{arccosh} \left(\frac{\gamma^{N-1} y_0 d}{2 \ln(\gamma) \xi} \right) - \tanh \left(\operatorname{arccosh} \left(\frac{\gamma^{N-1} y_0 d}{2 \ln(\gamma) \xi} \right) \right) \right. \\ \left. - \operatorname{arccosh} \left(\frac{\gamma^{1-N} y_0 d}{2 \ln(\gamma) \xi} \right) + \tanh \left(\operatorname{arccosh} \left(\frac{\gamma^{1-N} y_0 d}{2 \ln(\gamma) \xi} \right) \right) \right] \quad (\text{S27})$$

The radii of the mouth and tail of the pseudosphere are $R_{\text{mouth}}/d = \frac{\xi}{y_0 \gamma^{1-N} d}$, $R_{\text{tail}}/d = \frac{\xi}{\gamma^{N-1} y_0 d}$, respectively. Whenever $t_R/t_L = \gamma^2 \rightarrow 1$, both R_{mouth} and R_{tail} approach ξ/y_0 , and $(u_{N-1} - u_0)$ approaches $(N-1)d$. The pseudosphere reduces to a cylinder, as expected. In this limit, the HN model recovers the conventional tight-binding model with Hermitian tunnelings. We emphasize that, this visualization does not apply when either $R_{\text{mouth}} > R$ or $R_{\text{tail}} > R$, since ξ/y_0 sets a length scale for the pseudosphere. This is an analogue of that one can not find a circle on a sphere with its radius R_{circle} larger than the radius R of the sphere.

Lattice models leading to complex M

In the main text, we have shown that the mass M in the continuous model dual to the HN model changes from purely real to imaginary when the HN model goes across the exceptional point. In general, both t_L and t_R can be complex. We define $t_L = |t_L|e^{i\theta_L}$, $t_R = |t_R|e^{i\theta_R}$, and our approach gives the Schrödinger equation in the continuum, $-e^{i(\theta_L+\theta_R)/2} |t_L t_R|^{1/2} d^2 \left[\frac{2}{d^2} + \left(\frac{\partial}{\partial s} - q \right)^2 \right] \tilde{\psi}(s) = E \tilde{\psi}(s)$, where $q = \ln \left(\left| \frac{t_R}{t_L} \right|^{1/2} \right) \frac{1}{d}$, $\tilde{\psi} = e^{-i(\theta_R+\theta_L)s\frac{1}{2d}} \psi$. A coordinate transformation $\frac{y}{y_0} = e^{2qs}$ leads to

$$-e^{i(\theta_L+\theta_R)/2} |t_L t_R|^{1/2} d^2 \left[\frac{2}{d^2} + 4q^2 \left(y^2 \frac{\partial^2}{\partial y^2} + \frac{1}{4} \right) \right] \tilde{\psi}(y) = E \tilde{\psi}(y). \quad (\text{S28})$$

This equation describes a non-relativistic particle with a complex mass moving on a Poincaré half-plane. The mass term is $M e^{-i(\theta_L+\theta_R)/2}$. When $t_L, t_R \in \mathbb{R}$ but have opposite sign, $\theta_L + \theta_R = \pi$, such that the mass becomes purely imaginary, which recovers the result in the main text.

From the open boundary condition to the periodic one

The change from open to periodical boundary condition can be explored in both the HN model and its dual curved space. We define the HN model on a superlattice with the unit cell of N sites and use l to denote the lattice sites of this superlattice. We add an onsite potential V_L to the first lattice site of the unit cell, and consider a vanishing crystal momentum of the superlattice. Therefore, the Schrödinger equation is written as

$$-t_R\psi_{l,n-1} - t_L\psi_{l,n+1} + V_L\delta_{n,0}\psi_{l,n} = E\psi_{l,n}, \quad (\text{S29})$$

where $\psi_{l,N+1} = \psi_{l+1,0}$, $\psi_{l,-1} = \psi_{l-1,N-1}$. Since the crystal momentum of the superlattice is zero, we have $\psi_{l\pm 1,n} = \psi_{l,n}$. The general solution to the lattice model is $\gamma^n e^{ik_0 d}$, with eigenenergy $E(k_0) = -2\sqrt{t_R t_L} \cos(k_0 d)$. Since $E(k_0) = E(-k_0)$, a specific solution is written as $\psi = c_1 \gamma^n e^{ik_0 d} + c_2 \gamma^n e^{-ik_0 d}$. The boundary conditions

$$-t_R\psi_{l-1,N-1} - t_L\psi_{l,1} + V_L\psi_{l,0} = E\psi_{l,0}, \quad -t_R\psi_{l,N-2} - t_L\psi_{l+1,0} = E\psi_{l,N-1}, \quad (\text{S30})$$

leads to the following equation,

$$V_L/\sqrt{t_R t_L} = \frac{2 \sin(k_0 d)}{\sin(k_0 N d)} [\cosh(\ln(\gamma) N) - \cos(k_0 N d)]. \quad (\text{S31})$$

This equation determines $k_0 d$ as well as the spectrum and eigenstates of the lattice model. When $V_L/\sqrt{t_R t_L} \rightarrow \infty$, we have $k_0 d = m\pi/N$, $m \in \mathbb{Z}$. When $V_L = 0$, it solves $k_0 d = \pm i \ln(\gamma) + 2\pi m/N$, $m \in \mathbb{Z}$, where $c_2 = 0$ or $c_1 = 0$ if $k_0 d = +i \ln(\gamma) + 2\pi m/N$ or $k_0 d = -i \ln(\gamma) + 2\pi m/N$, respectively.

Utilizing the duality, we have the Schrödinger equation in the curved space,

$$-\frac{\hbar^2}{2M} \left(\frac{2}{d^2} \left(1 + \frac{1}{8} \kappa d^2 \right) + \kappa y^2 \frac{\partial^2}{\partial y^2} \right) \psi(y) + \sqrt{\kappa} d V_L y \sum_l \delta(y - Y_l) \psi(y) = E\psi(y), \quad (\text{S32})$$

where $Y_l = y_0 (\frac{y_N}{y_0})^l$ is the superlattice lattice site mapped on the Poincaré half-plane. The condition of zero superlattice crystal momentum exhibits itself by the discrete scaling symmetry in y -axis. The generic solution inside a unit cell of the superlattice is written as $y^{1/2+ik_y}$. Since the eigenenergy has $E(k_y) = E(-k_y) = \frac{\hbar^2}{2M} \left(-\frac{2}{d^2} + \kappa k_y^2 \right)$. We can write the specific solution $\psi(y) = c_1 y^{1/2+ik_y} + c_2 y^{1/2-ik_y}$. The boundary conditions

$$\psi_-(Y_l) = \psi_+(Y_l), \quad \psi'_+(Y_l) - \psi'_-(Y_l) = -\frac{2Md}{\hbar^2} \frac{V_L}{\sqrt{\kappa} Y_l} \psi(Y_l), \quad (\text{S33})$$

leads to the following equations

$$V_L / \left(\frac{\hbar^2}{2Md^2} \right) = \frac{2\sqrt{\kappa} k_y d}{\sin(\sqrt{\kappa} k_y N d)} \left[\cosh\left(\frac{\sqrt{\kappa} N d}{2}\right) - \cos(\sqrt{\kappa} k_y N d) \right]. \quad (\text{S34})$$

We would like to emphasize that in Eq. (S33) the effect of delta potential is related to $\frac{V_L}{\sqrt{\kappa} Y_l}$, which is also proportional to $\int_{Y_l^-}^{Y_l^+} \sqrt{g} dy \sqrt{\kappa} d V_L y \sum_l \delta(y - Y_l)$. Eq. (S34) shows the transition of spectrum also happens in the continuous model. We have $k_y = m\pi/(N\sqrt{\kappa} d)$ or $k_y = \pm \frac{i}{2} + 2m\pi/(N\sqrt{\kappa} d)$ for $V/\left(\frac{\hbar^2}{2Md^2}\right) \rightarrow \infty$ or $V = 0$, respectively. Similarly, we have $c_2 = 0$ for $k_y = \frac{i}{2} + 2m\pi/(N\sqrt{\kappa} d)$ and $c_1 = 0$ for $k_y = -\frac{i}{2} + 2m\pi/(N\sqrt{\kappa} d)$. We note that Eq. (S34) is exactly the same equation as Eq. (S31) in the lattice model if we take the limit of $k_0 d \rightarrow 0$.

Coupled HN chains

The lattice model illustrated in Fig. 3A of the main text reads

$$-t\Psi_{n,m+1} - t\Psi_{n,m-1} - t_R\Psi_{n-1,m} - t_L\Psi_{n+1,m} = E\Psi_{n,m}. \quad (\text{S35})$$

We define $\Psi(s, z)$ such that $\Psi(s_n, z_m) \equiv \Psi_{n,m}/d$, and $\Psi(s, z) = \Phi(s, z) e^{qs} e^{ik_0 s} e^{ik_{z0} z}$, where Φ is slowly varying. We have applied periodical boundary condition along the z -direction. Near the band bottom ($k_0 = 0, k_{z0} = 0$), substituting Ψ to Eq. (S35) and using the Taylor expansion of $\Phi(s, z)$, we obtain

$$-\left[(2t + t_R e^{-qd} + t_L e^{qd}) + (-t_R e^{-qd} + t_L e^{qd}) d \frac{\partial}{\partial s} + (t_R e^{-qd} + t_L e^{qd}) \frac{d^2}{2} \frac{\partial^2}{\partial s^2} + t d^2 \frac{\partial^2}{\partial z^2} \right] \Phi(s, z) = E\Phi(s, z) \quad (\text{S36})$$

A generic solution to this Schrödinger equation is written as $\Phi = e^{ik_ss}e^{ik_zz}$. We consider the periodic boundary condition in the z -direction. To ensure that the open boundary condition in s -direction and obtain an effective theory near $(k_0 = 0, k_{z0} = 0)$, we require $E(k_s, 0) = E(-k_s, 0)$, which leads to $-t_R e^{-qd} + t_L e^{qd} = 0$. The solution gives $q = \ln(\sqrt{t_R/t_L})/d$. For a finite k_z , the solution to Eq.(S36) that satisfies the boundary condition is written as $e^{ik_zz} \sin(k_ss)$. In other words, q and the resultant curvature, is independent of k_z .

After coordinate transformation $\frac{y}{y_0} = e^{2qs}$, Eq. (S36) is written as

$$-\left[2(t + \sqrt{t_L t_R}) + \sqrt{t_L t_R} d^2 \kappa \left(y^2 \frac{\partial^2}{\partial y^2} + \frac{1}{4}\right) + t d^2 \frac{\partial^2}{\partial z^2}\right] \Psi(y, z) = E \Psi(y, z), \quad (\text{S37})$$

where $\kappa = 4 \ln^2(\sqrt{\frac{t_R}{t_L}})/d^2$.

The model in Fig. 3B of the main text reads

$$-t\Psi_{n-1,m-1} - t\Psi_{n+1,m-1} - t\Psi_{n-1,m+1} - t\Psi_{n+1,m+1} - t_R\Psi_{n-1,m} - t_L\Psi_{n+1,m} = E\Psi_{n,m}. \quad (\text{S38})$$

The slowly varying $\Phi(s, z)$ satisfies

$$\begin{aligned} & -\left[\left(2te^{-qd} + 2te^{qd} + t_R e^{-qd} + t_L e^{qd}\right) + \left(-2te^{-qd} + 2te^{qd} - t_R e^{-qd} + t_L e^{qd}\right) d \frac{\partial}{\partial s} \right. \\ & \left. + \left(2te^{-qd} + 2te^{qd} + t_R e^{-qd} + t_L e^{qd}\right) \frac{1}{2} d^2 \frac{\partial^2}{\partial s^2} + 2t(e^{qd} + e^{-qd}) \frac{1}{2} d^2 \frac{\partial^2}{\partial z^2} + t(e^{qd} - e^{-qd}) d^3 \frac{\partial^2}{\partial z^2} \frac{\partial}{\partial s}\right] \Phi(s, z) = E\Phi(s, z). \end{aligned} \quad (\text{S39})$$

For effective theory near $(k_0 = 0, k_{z0} = 0)$, the open boundary condition in s -direction requires $E(k_s, 0) = E(-k_s, 0)$ and $-2te^{-qd} + 2te^{qd} - t_R e^{-qd} + t_L e^{qd} = 0$. This provides us with $q = \frac{1}{d} \ln\left(\sqrt{\frac{t_R+2t}{t_L+2t}}\right)$, and

$$-\left[2\tilde{t} + \tilde{t}d^2 \frac{\partial^2}{\partial s^2} + \frac{t}{\tilde{t}}(4t + t_L + t_R)d^2 \frac{\partial^2}{\partial z^2} + \frac{t}{\tilde{t}}(t_R - t_L)d^3 \frac{\partial^2}{\partial z^2} \frac{\partial}{\partial s}\right] \Phi(s, z) = E\Phi(s, z), \quad (\text{S40})$$

where $\tilde{t} = \sqrt{(t_R + 2t)(t_L + 2t)}$. When k_z is finite, the solution to Eq.(S40) reads $\Phi = e^{ik_zz} \sin(k_ss) e^{\left(\frac{t(t_R-t_L)}{2\tilde{t}^2} k_z d\right) k_z s}$. The extra exponential function gives rise to a k_z -dependent $q(k_z) = \frac{1}{d} \ln\left(\sqrt{\frac{t_R+2t}{t_L+2t}}\right) + \frac{td(t_R-t_L)}{2\tilde{t}^2} k_z^2$.

After coordinate transformation $\frac{y}{y_0} = e^{2qs}$ and $\Phi(s, z) = \Psi(s, z) e^{-qs}$, Eq. (S40) is written as

$$-\tilde{t}d^2 \left[\frac{2}{d^2} + \kappa_c \left(y^2 \frac{\partial^2}{\partial y^2} + \frac{1}{4} \right) + \frac{t(t_R - t_L)}{\tilde{t}^2} \frac{\partial^2}{\partial z^2} \left(\frac{4t + t_R + t_L}{t_R - t_L} + d\sqrt{\kappa_c} \left(y \frac{\partial}{\partial y} - \frac{1}{2} \right) \right) \right] \Psi(y, z) = E\Psi(y, z), \quad (\text{S41})$$

where $\kappa_c = \ln^2\left(\frac{t_R+2t}{t_L+2t}\right)/d^2$. A finite k_z modifies the curvature, $\kappa_c(k_z) = \ln^2\left(\frac{t_R+2t}{t_L+2t}\right)/d^2 + \frac{2t(t_R-t_L)}{\tilde{t}^2} \log\left(\frac{t_R+2t}{t_L+2t}\right) k_z^2 + O((k_z d)^4)$.

Whereas the above discussions apply to the band bottom, the effective theory can be formulated at any energy. In the lattice models, we write $\Psi_{n,m} = \psi_n e^{ik_{z0}md}$, and obtain

$$-2t \cos(k_{z0}d) \psi_n - t_R \psi_{n-1} - t_L \psi_{n+1} = E\psi_n, \quad (\text{S42})$$

and

$$-(t_R + 2t \cos(k_{z0}d)) \psi_{n-1} - (t_L + 2t \cos(k_{z0}d)) \psi_{n+1} = E\psi_n, \quad (\text{S43})$$

for Eq. (S35) and (S38), respectively. Therefore, for each k_{z0} , we have a dual model in the curved space. Especially, for Eq. (S38), we obtain a k_{z0} -dependent HN model and the corresponding curved space can be derived in the same manner as in the main text, where $\kappa = \ln^2\left(\left|\frac{t_R+2t \cos(k_{z0}d)}{t_L+2t \cos(k_{z0}d)}\right|\right)/d^2$, which is k_{z0} dependent. It reduces to κ_c if we take the limit of $k_{z0}d \rightarrow 0$.

* They contribute equally to this work.

[†] zhou753@purdue.edu

- [1] M. C. Gutzwiller, Stochastic behavior in quantum scattering, *Physica D: Nonlinear Phenomena* **7**, 341 (1983).
- [2] S. Yao and Z. Wang, Edge states and topological invariants of non-hermitian systems, *Phys. Rev. Lett.* **121**, 086803 (2018).
- [3] K. Yokomizo and S. Murakami, Non-bloch band theory of non-hermitian systems, *Phys. Rev. Lett.* **123**, 066404 (2019).
- [4] Z. Yang, K. Zhang, C. Fang, and J. Hu, Non-hermitian bulk-boundary correspondence and auxiliary generalized Brillouin zone theory, *Phys. Rev. Lett.* **125**, 226402 (2020).